ISSN 0022-4766, Journal of Structural Chemistry, 2025, Vol. 66, No. 5, pp. 877-888. © Pleiades Publishing, Ltd., 2025.
Text © The Author(s), 2025, published in Zhurnal Strukturnoi Khimii, 2025, Vol. 66, No. 5, 143910.

SYNTHESIS AND STRUCTURAL CHARACTERIZATION OF A NOVEL TERNARY COMPOSITE CONTAINING xLiFeO$_2$, yLi$_3$V$_2$(PO$_4$)$_3$, AND (1 – x – y)LiCoO$_2$ COMPOSITES FOR LITHIUM-ION BATTERIES (LIBs)

M. Monajjemi[1]* and F. Mollaamin[2]

The objective of this research is to prepare a composite with lower cost and better cyclability than the other cathode materials in lithium-ion battery. A ternary composition with high efficiency and low cost containing $LiFeO_2$ and $Li_3V_2(PO_4)_3$ (LVP), was applied instead of pure $LiCoO_2$ to reduce usage of a percentage Co amount, consequently reducing the cost of cobalt and removing its toxic effect in LIBs. In this study, we synthesized ten samples from mixture of xLiFeO$_2$, yLi$_3$V$_2$(PO$_4$)$_3$, and (1 – x – y)LiCoO$_2$ compounds for preparing a suitable cathode electrode with high initial discharge capacity, large cyclability and inexpensive cost instead of traditional cathode materials. As a result by using Raman analysis, X-ray diffraction, and electrochemical analyzing, we found that the $Li_{1.67}V_{0.67}$ $Fe_{0.33}$ $Co_{0.33}$ [$(PO_4)_3$,O_2] composites have high efficiency and best performance in viewpoint of initial capacity, cyclability, charge and discharge capacities among these ten composites.

DOI: 10.1134/S0022476625050014

Keywords: lithium-ion batteries, cathode materials, $Li_3V_2(PO_4)_3$, $LiFeO_2$, $LiCoO_2$, ternary composites.

INTRODUCTION

$Li_3V_2(PO_4)_3$ (LVP) is an important material applying for cathode in LIBs, which consists of both mobile lithium ions and redox metal ions including a rigid phosphate structure. In viewpoint of electrochemical and thermal have high stability, high operating potential and safety. This molecule consists of two crystal structures known as 1-rhombohedral and 2-monoclinic including a PO_4 tetrahedral, which is attached to the VO_6 octahedral in different forms. The solid powder $Li_3V_2(PO_4)_3$ was synthesized for the first time via Rietveld refinements [1]. In addition, lithium extraction out of the monoclinic form of $Li_3V_2(PO_4)_3$ was presented by Barker and Saidi [2] and Sato et al. [3], with the crystal structure of the space group $P2_1/n$ with lattice parameters as a = 8.598 Å, b = 8.593 Å, c = 12.033 Å, α = 92.0°, β = 91.5° and γ = 90.5° based on Fu et al. calculation [4]. Figure 1 exhibits the detailed bonding atoms a surrounding of phosphorus through tetrahedral structure with 4 oxygen atoms, as well as vanadium, which create an octahedral structure with 6 oxygen atoms.

Herein, we report a structure tracking-aided design and synthesis of single-crystal $Li_3V_2(PO_4)_3$ (LVP) nanoparticles using X-ray spectroscopy and imaging techniques according to thermodynamics and kinetics of synthesis reactions.

[1]Department of Chemical Engineering, Central Tehran Branch, Islamic Azad University, Tehran, Iran; *maj.monajjemi@iauctb.ac.ir; m_monajjemi@yahoo.com. [2]Department of Biomedical Engineering, Faculty of Engineering and Architecture, Kastamonu University, Kastamonu, Türkiye. Original article submitted September 4, 2024; revised December 27, 2024; accepted January 1, 2025.

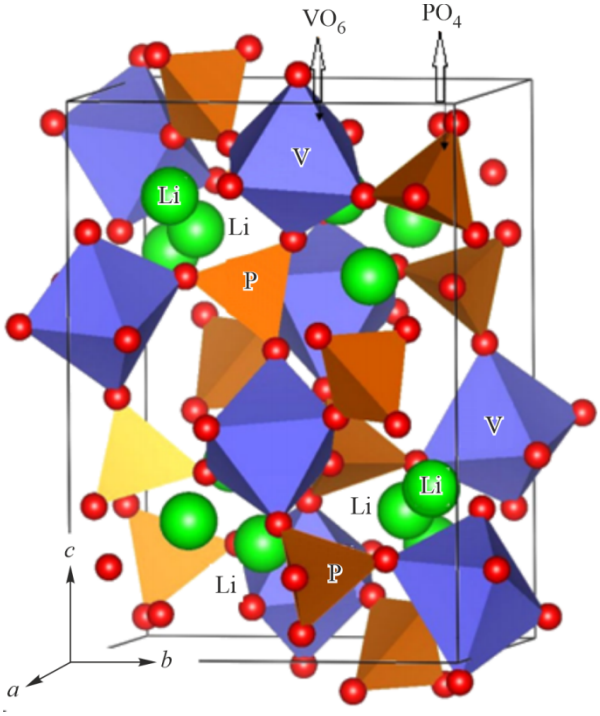

Fig. 1. Li_3V_2 $(PO_4)_3$ structure based on group theory model of ($P2_1/n$).

Designing of a cost-efficient synthesis protocol for making nano-crystalline LVP is a crucial step leading to an amorphous intermediate with local structural ordering resembling that of LVP. The obtained LVP particles between 5-50 nm coated with thin layer of amorphous carbon and featured with excellent cycling stability and rate capability. In addition to the traditional olivine-based metal phosphates (i.e., Li$M$$PO_4$; M = Fe, Mn), lithium vanadium phosphate, $Li_3V_2(PO_4)_3$ (LVP) has emerged as a promising cathode material due to its abundance, high thermal stability and capability of delivering high capacity at high working potentials (~4 V). Between the two polymorphs of LVP, i.e., rhombohedral and monoclinic phases, the latter is thermodynamically stable and preferable for the use as high-energy and high-power cathodes owing to its three-dimensional open framework for fast lithium-ion diffusion and accommodating [2-4].

Since LVP by its unique crystal combination as well as with high thermodynamic stability creates a suitable situation among the cathode materials, wide interest due to its high lithium diffusion coefficient appears for researchers, which has more advantage over traditional cathode materials such as $LiCoO_2$ [5, 6]. Vanadium in LVP structure due to its lower environmental destruction and also less toxic material causes to increase its ability to use in a wide range of diverse applications [7, 8]. The necessity of lithium diffusion in electrolytes, which increases the rate of activities of charged and discharged is an important item for combination of this material with other materials such as $LiFeO_2$ and $LiCoO_2$ for synthesizing a targeted composites for cathode materials for our research work. Since in the solid-state electrolytes diffusion of Li ions from electrodes towards electrolytes by a low concentration appears in any type of LIBs, pores structure of the $x$$LiFeO_2$, $y$$Li_3V_2(PO_4)_3$, and $(1-x-y)$$LiCoO_2$ composites electrodes could be caused higher rate of Li^+ ion diffusion in these types of electrolytes [9-11]. In other hand, regarding to lithium iron oxides, which are considered to have low cost and non-toxicity, they are one of the best products for applying as a cathode of lithium secondary battery for combination with $Li_3V_2(PO_4)_3$. As an alternate cathode material, $LiFeO_2$ has used widely due to its abundant raw materials, low cost, and non-toxicity [12, 13]. $LiFeO_2$ has also been made wide advances on its application, and optimization due to extensive benefit of novel preparation methods, with accurate analysis through Mossbauer spectra, HRTEM, etc. [14, 15]. Since $LiFeO_2$ has several structural shapes, (α, β, and γ) [16, 17], we used α-$LiFeO_2$ in our work due to amazing electrochemical properties [18]. According to the properties of these compounds, $x$$LiFeO_2$, $y$$Li_3V_2(PO_4)_3$, and $(1-x-y)$$LiCoO_2$ composites electrodes

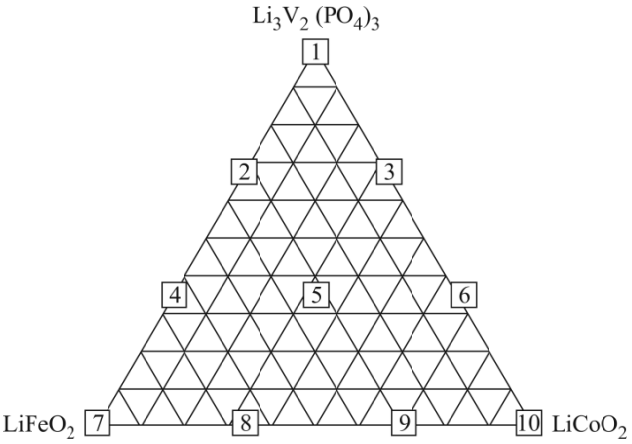

Fig. 2. Binary and ternary diagram of xLiFeO$_2$, yLi$_3$V$_2$(PO$_4$)$_3$, and $(1-x-y)$LiCoO$_2$ composites with 10 samples.

TABLE 1. 10 Composites Structure Based on Lever Rule from Triangle Diagram

Sample	Composites
1	$Li_3V_2(PO_4)_3$
2	$Li_{2.33}V_{1.33}Fe_{0.33}[(PO_4)_3,O_2]$
3	$Li_{2.33}V_{1.33}Co_{0.33}[(PO_4)_3,O_2]$
4	$Li_{1.67}V_{0.67}Fe_{0.67}[(PO_4)_3,O_2]$
5	$Li_{1.67}V_{0.67}Fe_{0.33}Co_{0.33}[(PO_4)_3,O_2]$
6	$Li_{1.67}V_{0.33}Co_{0.67}[(PO_4)_3,O_2]$
7	$LiFeO_2$
8	$LiFe_{0.67}Co_{0.33}O_2$
9	$LiFe_{0.33}Co_{0.67}O_2$
10	$LiCoO_2$

can make excellent impact on the electrochemical performance of cathodes. In this work, we prepared ten compositions of binary and ternary solid solutions, including xLiFeO$_2$, yLi$_3$V$_2$(PO$_4$)$_3$, and $(1-x-y)$LiCoO$_2$ composites (Fig. 2).

By this method, we tried to prepare a suitable cathode electrode containing combination materials of several composites consisting of xLiFeO2, yLi$_3$V$_2$(PO$_4$)$_3$, and $(1-x-y)$LiCoO$_2$ systems with high initial discharge capacity, large cyclability. Therefore, initially, several composition points (10 items) according the lever rule, stoichiometric weights and mole-fractions were selected to prepare a cathode material with good electrochemical performance. The mole fractions of these 10 points were yielded through the triangle phase diagram and then were synthesized via sol-gel method (Table 1). As it can be observed in the Fig. 2 and Table 1, vanadium and lithium amounts are decreased towards down direction of triangle; in contrast the compositions of **7-10** have zero vanadium concentration.

The objective of this research is to prepare a composite with lower cost and better cyclability than the other cathode materials in lithium-ion battery. We believe that this topic for study was accomplished due to the first novel report of the mechanical and physical properties of commercially available composites consisting of xLiFeO$_2$, yLi$_3$V$_2$(PO$_4$)$_3$, and $(1-x-y)$LiCoO$_2$ systems and these experimental data are important for increasing the cycle life and can be used as a cathode material. By this work, we also predicted and confirmed that Fe substitution would lead to a lower potential at the end of charge. Both XPS and first principles electronic structure computations indicate that Ni and Fe are simultaneously oxidized in this material. Computations further indicate that Co will only be oxidized at the very end of charge. In this work,

we have demonstrated that the results of this experiment have produced a new electrode material with very few iteration steps in the material design cycle.

EXPERIMENTAL

Synthesized and characterizations of $Li_3V_2(PO_4)_3$. Penta oxide vanadium (99.6%, Alfa Aesar), phosphate di-hydrogen ammonium ($NH_4H_2PO_4$, 99.5%, Sigma-Aldrich), oleic acid (FCC, FG, Aldrich), oxalic acid (99.5%, Sigma-Aldrich), lithium acetate ($LiCOOCH_3{\cdot}2H_2O$, reagent grade, Sigma), and paraffin wax (ASTMD 87, melting point 50-60 °C, Aldrich) were provided. At first, 1:2 mole fraction of V_2O_5 with oxalic acid in were mixed into deionized water and completely stirred at 298 K to reach a clear blue solution. The product of $VOC_2O_4{\cdot}nH_2O$ has been produced and then H_2O was evaporated from the solution. For $Li_3V_2(PO_4)_3$ nano-belt synthesis, $LiCOOCH_3{\cdot}2H_2O$, $VOC_2O_4{\cdot}nH_2O$ $NH_4H_2PO_4$, oleic acid, and paraffin wax were used as precursors. Phosphate di-hydrogen ammonium and oleic acid were milled together with for 1.5 h in a high-speed miller (SPEX 8000 M), and then the mixture with paraffin wax was milled for 0.5 h more. Consequently, the VOC_2O_4 solution and lithium acetate were added to the mixture and mixture was milled for 20 min. In total, lithium, vanadium, phosphate, and oleic acid molar ratio of the stoichiometric in the mixture was 3:2:3:3. Final product as a viscous liquid slurry was dried in an oven over 120 °C for 1 h and then heated at high temperature between 75-850 °C for 5 h under a glove box to produce the final $Li_3V_2(PO_4)_3$ nanostructures. The crystalline atoms position of $Li_3V_2(PO_4)_3$ was confirmed by X-ray diffraction (XRD) analysis, using a Scintag XDS 2000 powder diffractometer equipped with a Ge (Li) solid-state detector (Fig. 3*a*).

The SEM image indicates that prepared product has a granular structure with average grain size of a few micrometers. TEM measurements were accomplished on a JEOL 2100F operated at 220 kV. The powder of $Li_3V_2(PO_4)_3$ with an amorphous carbon was dispersed on a TEM holder and then moved to the TEM column (Fig. 3*b*). Cathode electrode was prepared by slurry of 65 wt.% activated products, 25 wt.% super-P carbon, and 10 wt.% kynar binder on the aluminum foil.

Synthesized, Characterizations of α-$LiFeO_2$. We prepared the α-$LiFeO_2$ nano structure through a simple, fast and unique strategy by a low temperature calcined process as follows: an amount of 2.8 g hydroxide lithium ($LiOH{\cdot}H_2O$) (Merck, Germany) and 4 g of $Fe(NO_3)_3{\cdot}9H_2O$ (Merck, Germany) was dissolved in 25 mL C_2H_5OH. The mixture was washed several times by distilled water and ethanol alternately to remove redundant LiOH, consequently the brown mixture was dried at 90 °C for 15 h in an argon glove box. Finally, the mixture was heated at temperatures 400 °C for 5 h in glove box under argon gas. The product was characterized via XRD (DX-1000, Bruker, Karlsruhe, Germany, CuK_α radiation) (Fig. 4). Raman was done by a Jobin Yvon Horiba, model T64000 and the quantitative analysis was performed by the thermogravimetric analyzer (TGA, Mettler Toledo: TGA/DSC 3+ HT1600).

Powders morphology of α-$LiFeO_2$ was analyzed using scanning electron microscope (SEM) (SU3900, Hitachi, Ltd., Tokyo, Japan) and the HT7800 RuliTEM transmission electron microscope (TEM) (HT7800, Hitachi, Ltd., Tokyo, Japan) (Fig. 5).

The active center area and pore volume were calculated by Brunauer–Emmett–Teller (BET) (N2 V-Sorb 2800P BET surface area and micro-pore analyzer, China). The cathode electrode was manufactured with 83% synthesized product, 12% acetylene black, and 5% polyvinylidene fluoride binder in N-methyl-2-pyrrolidone solvent. The slurry was compressed inside an aluminum foil and dried at 120 °C for 5 h. Finally, composites preparation, characterization, cathode assembly, cell assembly and electro-chemical testing were accomplished and tested for 10 samples containing $x$$LiFeO_2$, $y$$Li_3V_2(PO_4)_3$, and $(1-x-y)$$LiCoO_2$. The objective of this research is to find a ternary composition with low-cost materials for reducing the amount weight of cobalt and removing its toxic effect in cathode materials of LIBs.

Preparation and characterization of 10 samples containing $x$$LiFeO_2$, $y$$Li_3V_2(PO_4)_3$, and $(1-x-y)$$LiCoO_2$ for cathode material electrodes. All the 10 samples were prepared using the sol-gel synthesis method. Sol-gel method was basically applied due to the chemical reaction is fast and easy for these ternary systems compared with the conventional

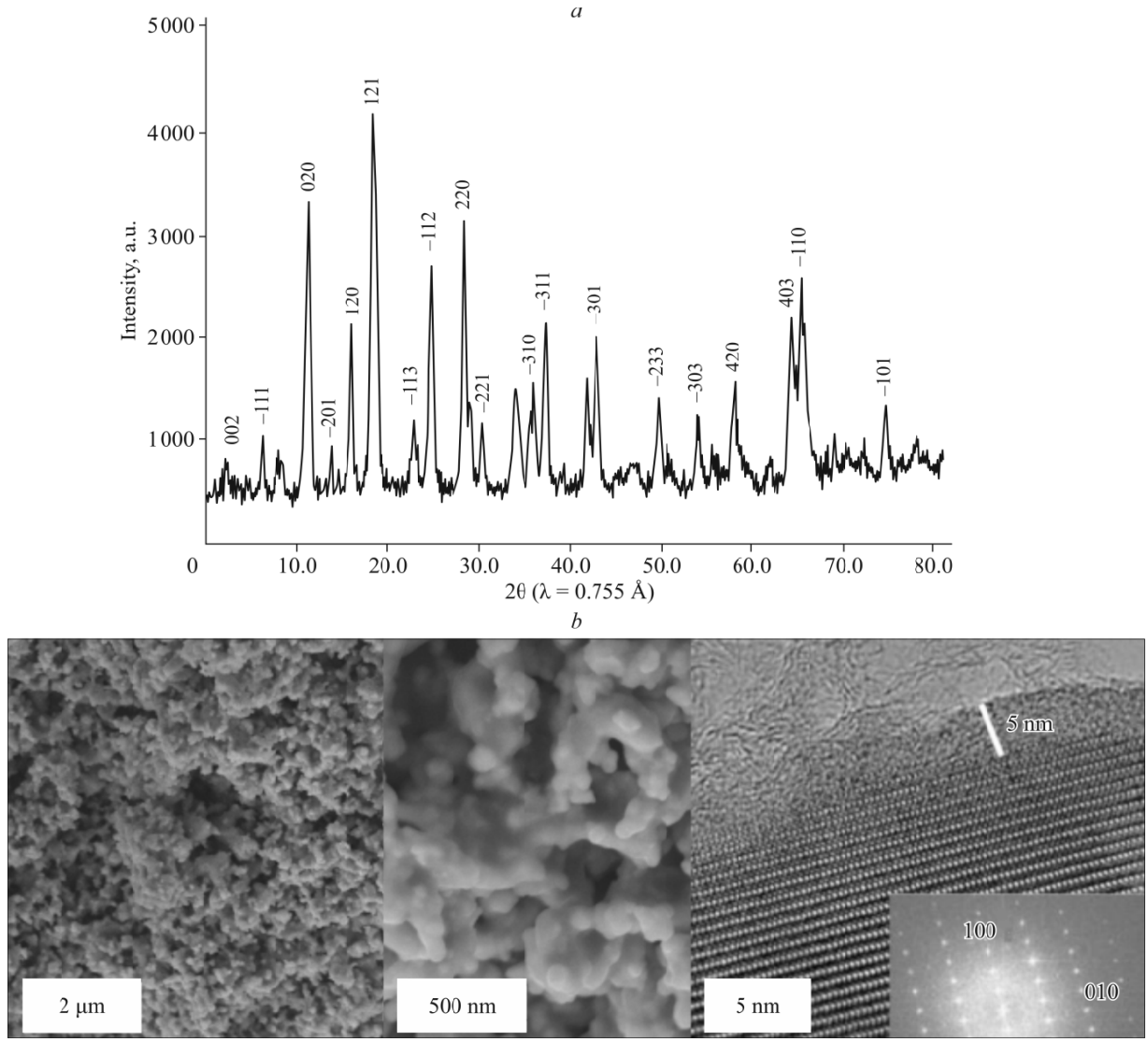

Fig. 3. XRD pattern of the $Li_3V_2(PO_4)_3$/C synthesized sample (*a*); SEM & high-resolution TEM image of $Li_3V_2(PO_4)$ (*b*).

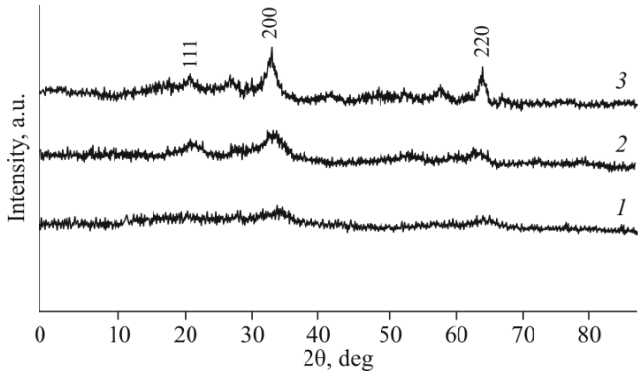

Fig. 4. XRD patterns of the α-$LiFeO_2$ at 80 ℃ (*1*); 120 ℃ (*2*); 180 ℃ (*3*).

solid-state synthesis. Particularly, it can be done with a low reaction temperature and also has a high degree of homogeneity in their morphologies.

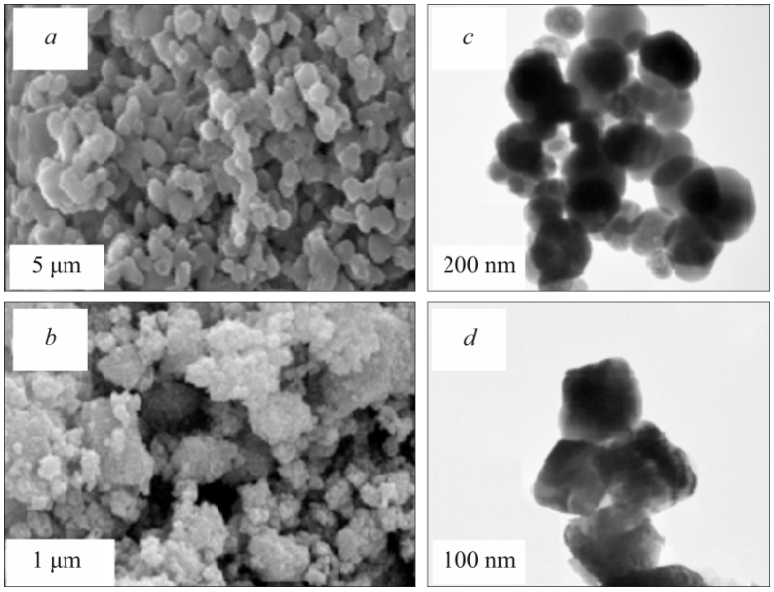

Fig. 5. Typical SEM (*a*, *b*) and TEM (*c, d*) images of α-$LiFeO_2$ samples.

Although one of the best methods for synthesizing mixed layered oxides of lithium and several transition metals is the method of co-precipitation of the corresponding hydroxides from solution using precipitating agents to achieve the required degree of homogeneity, this method was used mostly for preparation of a double layered composites (our systems are multi-layered). In addition, layered double hydroxides (LDHs) have mostly received considerable attention due to their properties and potential applications as catalysts, catalyst precursors or catalyst support, adsorbents, and anion exchangers, while in our systems the potential of cathode materials for 10 samples in viewpoint of cyclability, high charging were considered. Another important reason that we used sol-gel method instead of co-precipitation of the corresponding hydroxides from solution is due to lack of pH values for our work, while these values are important for co-precipitation method. Finally, complexity for synthesis of ten samples with the mentioned structures in Table 1 enforced us to use simple sol-gel method for our composites. Since this method makes it possible to obtain various composites, especially in the form of submicron powders, all 10 samples were prepared using the sol-gel synthesis method including stoichiometry weights of each compounds of $x$$LiFeO_2$, y$Li_3V_2(PO_4)_3$, and $(1 - x - y)$$LiCoO_2$.

In the whole ternary diagram (Table 2, Fig. 2) 10 specific points were selected to find suitable regions and trends in capacity and cyclability. The perpendicular line for each end point exhibits the percentage of one of the ternary present. As

TABLE 2. Capacity and Cyclability for 10 Samples, of the System $x$$LiFeO_2$, $y$$Li_3V_2(PO_4)_3$, and $(1 - x - y)$$LiCoO_2$

Sample	Blend	$LiFeO_2$	$LiCoO_2$	$Li_3V_2(PO_4)_3$	Capacity	Cyclability
1	Pure	0	0	1	160.5	88
2	Binary	0.33	0	0.67	93.2	45
3	Binary	0	0.33	0.67	94.4	41
4	Binary	0.67	0	0.33	103.4	55
5	Ternary	0.33	0.33	0.33	178.8	89
6	Binary	0	0.67	0.33	89.9	62
7	Pure	1	0	0	160.3	80
8	Binary	0.833	0.167	0	179.5	49.7
9	Binary	0.167	0.833	0	105.4	61
10	Pure	0	1	0	145.3	83

instance, for $LiCoO_2$ the red line demonstrates its amount and reduces from 1 to 0 as the line moves away from $LiCoO_2$ towards the other corners of the diagram. Table 2 exhibits the percentage material compositions of all 10 samples. See papers [19, 20] and also References [21-30] for better understanding of characterization techniques and what information we get from these techniques.

RESULTS

Raman analyzing. This test has been done for all 10 composites to confirm the combination morphologies in proper phases of materials listed in Table 2. Raman spectroscopy was used to predict the structure and cathode material properties of 10 samples. Fig. 6 exhibits spectra of the pure $LiFeO_2$ and $LiCoO_2$ and also $x LiFeO_2$, $y Li_3V_2(PO_4)_3$, and $(1-x-y)LiCoO_2$ including samples **2**-**5** from Table 2. The highest peak at 990 cm^{-1} belongs to $Li_3V_2(PO_4)_3$ in structures with group theory model of $P2_1/n$ (Fig. 1). Although the peaks of pure $LiFeO_2$ and $LiCoO_2$ are 485 cm^{-1} and 590 cm^{-1}, respectively, but these amounts will change a little bit in mixture samples of $x LiFeO_2$, $y Li_3V_2(PO_4)_3$, and $(1-x-y)LiCoO_2$. The peaks widths indicate a stability of those samples due to uncertainty principle of Heisenberg rule. Although the position and the place of Raman peaks do not change with percentage of samples, the amounts of peaks are changed that is a factor for recognition of each sample.

X-ray. Although X-ray diffraction was done for all 10 items, inductively coupled plasma atomic emission spectroscopy (ICP-AES) characterization methods were only done on the composites that exhibited correct results and were checked several times. XPS (CuK_α radiation with $\lambda = 1.55$ Å) was done to have a precise analysis about the percentage amount and the oxidation states of the iron, vanadium, and cobalt to verify the exact composition of the samples (Fig. 3, 4, and 7). The θ angles for the composites with sharp peaks were observed based on Bragg's law to recognize the existence of any unknown substances via diffraction data (Table 3). Moreover, the plasma spectroscopy (ICP-AES) method has been applied to identify transition metals in the compositions of 10 samples (ICP analyzers; PerkinElmer Optima 7300 DV containing Cetac ASX-520 auto sampler).

Electrochemical testing and analyzing. The electrochemical efficiency of these samples as cathode materials was tested using Arbin BT2000 and MITS Pro Arbin software. The cycling was done between 2.5 V up to 4.5 V with constant *C*-rate of *C*/12 at 298 K. Figure 8 exhibits the initial charge-discharge curves among these voltages (V) and capacities (mAh/g). All figures have drawn in identical scale for any further comparison among the samples.

Samples **2**-**4** (Fig. 8*a*) have exhibited a lower capacity retention. The capacities were found to be in ascending order for samples **1**-**4**, which means that end member $Li_{1.67}V_{0.67}Fe_{0.67}[(PO_4)_3,O_2]$ exhibited a significant deleterious effect on their

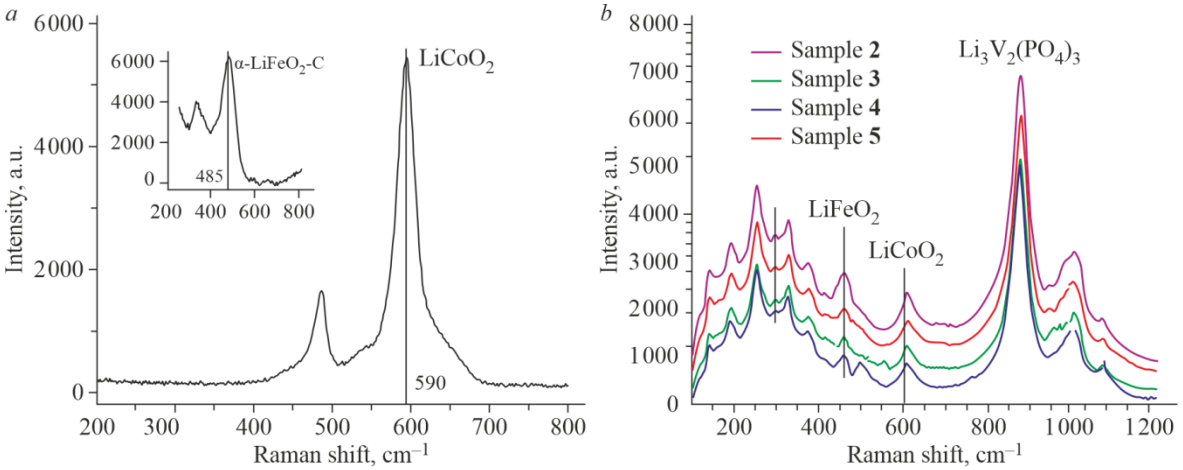

Fig. 6. Raman spectra: pure $LiFeO_2$ and $LiCoO_2$ (*a*); $x LiFeO_2$, $y Li_3V_2(PO_4)_3$, and $(1-x-y)LiCoO_2$ (*b*) contain samples **2**-**5** from Table 2.

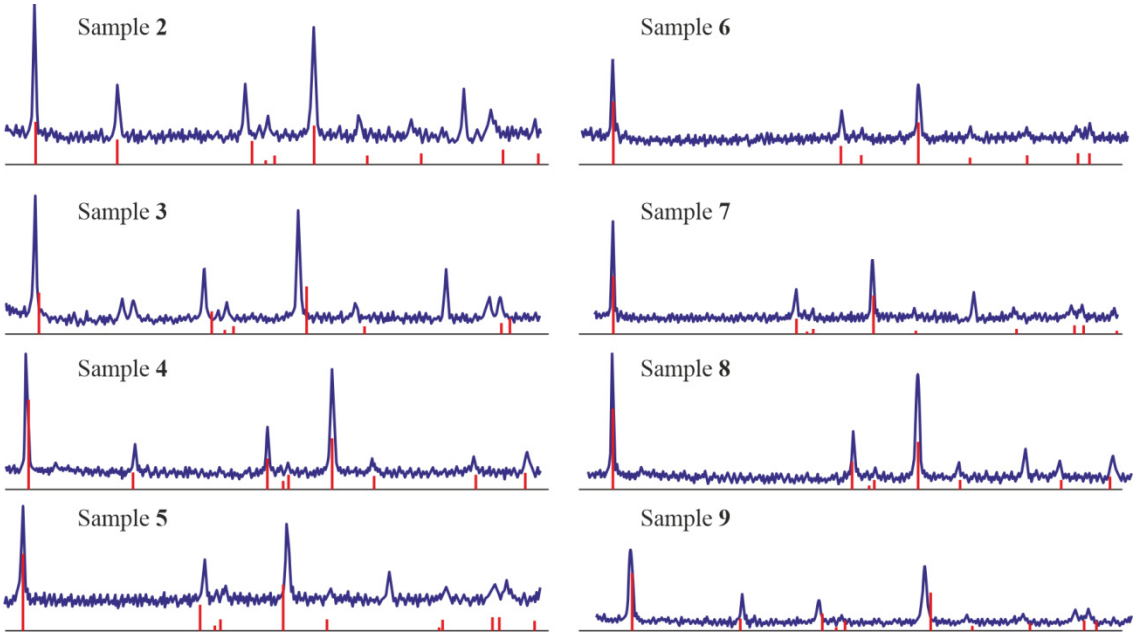

Fig. 7. XRD plots of samples **2-9** from the current system.

TABLE 3. Lattice Parameters of Composites (nm)

Sample	*a*	*b*	*c*
2	0.2355	0.3423	1.06
3	0.2188	0.2354	1.13
4	0.3424	0.3277	1.32
5	0.1734	0.2435	1.09
6	0.3421	0.3243	1.11
7	0.2359	0.2541	1.52
8	0.2654	0.2632	1.22
9	0.3288	0.2244	1.34

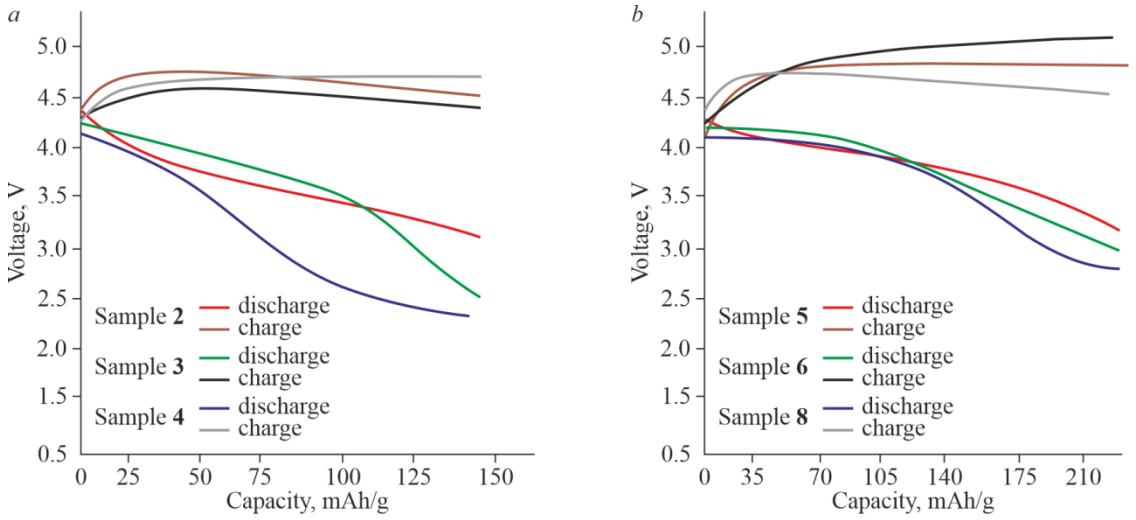

Fig. 8. Initial charge-discharge: **2-4** samples (*a*); **5**, **6**, and **8** samples (*b*).

capacities. Samples **5-8** (Fig. 8*b*) have better capacity and cyclability properties than the rest of them, particularly the sample **5**. In addition, the sample **5** is located in the center of the ternary composition triangle and it has suitable amount of capacity. Samples **6**, **8** exhibit good capacity retention, but low-capacity amounts.

DISCUSSION

This investigation is designed for preparing the best cathode material composition from ternary systems of $x\text{LiFeO}_2$, $y\text{Li}_3\text{V}_2(\text{PO}_4)_3$, and $(1-x-y)\text{LiCoO}_2$ with high initial discharge capacity, large cyclability and inexpensive cost material. Therefore, firstly, 10 different composition points using the lever rule, stoichiometric weights and mole-fractions were selected for finding an excellent cathode material including high electrochemical efficiency. The combination of these 10 composites was calculated through the triangle phase diagram (Fig. 2, Table 2), and then synthesis based on above mentioned methods was fulfilled. Vanadium amount is decreased towards down direction of triangle; meanwhile the compositions of **7-10** have zero vanadium percentage. High amount of vanadium is found at the sample **1**. Obviously, the most amount of cobalt can be found at the sample **10** and its various percentages can be found in a wide region in the triangle, which are zero in samples **1**, **2**, **4**, and **7**. It is notable, that the capacity and cyclability of each sample is strongly dependent on the amount values of vanadium, cobalt, and Fe concentration in the composites. In addition, any specific capacitance can be extracted from the number of energies (reserve with volume or mass, Ah), while the rate capability should be extracted only from the cell during charging. Therefore, the *C*-rate is the capacity of the cell segregated by the hourly charging rate. The discharge capacity plots have been measured with 18650-type C/LiCoO_2 Sony battery result which is modified by Ehrlich [31, 32]. The samples were measured via a cycler (Arbin BT 2000 battery testing instrument), between 2.5 V and 4.5 V with low *C*-rate of *C*/12. The initial discharge capacities varied from 89.9 mAh/g to 179.5 mAh/g. Although the sample 8 exhibits high capacity of 179.5 mAh/g, it contains low cyclability. Therefore, the sample 5 has more suitable composition due to the capacity and cyclability compared with other items (Fig. 9).

Table 4 summarizes the initial charge /discharge and retention percentage for all 10 composites in the system of $x\text{LiFeO}_2$, $y\text{Li}_3\text{V}_2(\text{PO}_4)_3$, and $(1-x-y)\text{LiCoO}_2$. Four of 10 samples exhibited discharge more than 160 mAh/g in which the sample **8** exhibited the highest capacity and 100% retention between 2.5 up to 4.5 voltage range. It is worthy to note that composites having mixed amount of Fe and Co exhibited good results in comparison to alone vanadium or alone cobalt based materials, therefore giving the possibility of cost advantages.

Motivated by a series of experiments on 10 composites with Co, Fe, Ni and Mn substituted in cathode materials synthesized by a sol-gel method, we predicted and confirmed that Fe and Ni substitution would lead to a lower potential at the end of charge. Both XPS and first principles electronic structure computations indicate that Ni and Fe are simultaneously oxidized in this material. Results indicate that Co will only be oxidized at the very end of charge. Using Raman analysis,

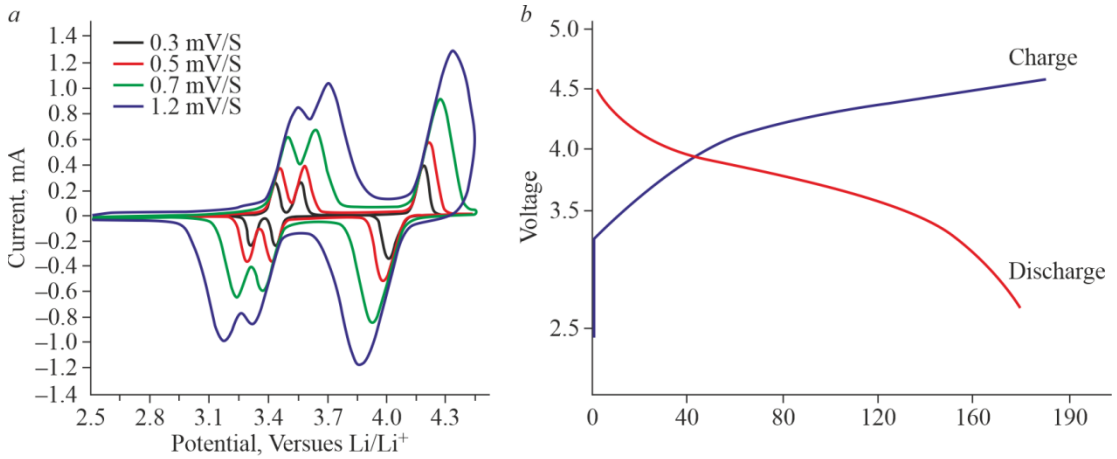

Fig. 9. Current versus Li /Li^+ for sample **5** (*a*); capacity and cyclability for sample **5** (*b*).

TABLE 4. Initial charge /discharge and retention percentages of all composites build up by xLiFeO$_2$, yLi$_3$V$_2$(PO$_4$)$_3$, and $(1 - x - y)$LiCoO$_2$

No.	Sample composition	Charge (mAh/g)	Discharge (mAh/g)	Retention (%)
1	$Li_3V_2\ (PO_4)_3$	200.3.4	160.5	82.5
2	$Li_{2.33}V_{1.33}\ Fe_{0.33}[(PO_4)_{3,}O_2]$	155.8	93.2	89.5
3	$Li_{2.33}V_{1.33}\ Co_{0.33}[(PO_4)_{3,}O_2]$	149.3	94.4	81.6
4	$Li_{1.67}V_{0.67}\ Fe_{0.67}[(PO_4)_{3,}O_2]$	153.2	103.4	83.4
5	$Li_{1.67}V_{0.67}\ Fe_{0.33}\ Co_{0.33}[(PO_4)_{3,}O_2]$	240.5	178.8	100
6	$Li_{1.67}V_{0.33}\ Co_{0.67}[(PO_4)_{3,}O_2]$	154.8	89.9	90.4
7	$Li\ FeO_2$	201.3	160.3	89.2
8	$Li\ Fe_{0.67}\ Co_{0.33}\ O_2$	223.6	179.5	100
9	$Li\ Fe_{0.33}\ Co_{0.67}\ O_2$	165.3	105.4	91.5
10	$Li\ CoO_2$	238.5	145.3	87.5

X-ray diffraction, and electrochemical analyzing, we found that the $Li_{1.67}V_{0.67}\ Fe_{0.33}\ Co_{0.33}\ [(PO_4)_3,\ O_2]$ composites have high efficiency and best performance in viewpoint of initial capacity, cyclability, charge and discharge capacities among these ten composites.

FUNDING

This work was supported by ongoing institutional funding. No additional grant to carry out or direct this particular research were obtained.

CONFLICT OF INTERESTS

The authors of this work declare that they have no conflicts of interest.

REFERENCES

1. H. M. Rietveld. A profile refinement method for nuclear and magnetic structures. *J. Appl. Crystallogr.*, **1969**, *2*(2), 65-71. https://doi.org/10.1107/s0021889869006558
2. J. Barker and M. Y. Saidi. Lithium-Containing Phosphates, Method of Preparation, and Uses Thereof. US Patent 6203946, **2001**.
3. M. Sato, H. Ohkawa, K. Yoshida, M. Saito, K. Uematsu, and K. Toda. Enhancement of discharge capacity of $Li_3V_2(PO_4)_3$ by stabilizing the orthorhombic phase at room temperature. *Solid State Ionics*, **2000**, *135*(1-4), 137-142. https://doi.org/10.1016/s0167-2738(00)00292-7
4. P. Fu, Y. Zhao, Y. Dong, and X. Hou. Synthesis of high tap density $Li_3V_2(PO_4)_3$ cathode materials using mixed lithium precursors. *J. Phys. Chem. Solids*, **2010**, *71*(3), 394-399. https://doi.org/10.1016/j.jpcs.2010.01.009
5. J.-C. Zhang, Z.-D. Liu, C.-H. Zeng, J.-W. Luo, Y.-D. Deng, X.-Y. Cui, and Y.-N. Chen. High-voltage $LiCoO_2$ cathodes for high-energy-density lithium-ion battery. *Rare Met.*, **2022**, *41*(12), 3946-3956. https://doi.org/10.1007/s12598-022-02070-6
6. R. Konar, S. Maiti, N. Shpigel, and D. Aurbach. Reviewing failure mechanisms and modification strategies in stabilizing high-voltage $LiCoO_2$ cathodes beyond 4.55 V. *Energy Storage Mater.*, **2023**, *63*, 103001. https://doi.org/10.1016/j.ensm.2023.103001

7. Y. Shi, H. Zhou, I. D. Seymour, S. Britto, J. Rana, L. W. Wangoh, Y. Huang, Q. Yin, P. J. Reeves, M. Zuba, Y. Chung, F. Omenya, N. A. Chernova, G. Zhou, L. F. J. Piper, C. P. Grey, and M. S. Whittingham. Electrochemical performance of nanosized disordered $LiVOPO_4$. *ACS Omega*, **2018**, *3*(7), 7310-7323. https://doi.org/10.1021/acsomega.8b00763
8. Y.-S. Duh, X. Liu, X. Jiang, C.-S. Kao, L. Gong, and R. Shi. Thermal kinetics on exothermic reactions of a commercial $LiCoO_2$ 18650 lithium-ion battery and its components used in electric vehicles: A review. *J. Energy Storage*, **2020**, *30*, 101422. https://doi.org/10.1016/j.est.2020.101422
9. B. Ramasubramanian, S. Sundarrajan, V. Chellappan, M. V. Reddy, S. Ramakrishna, and K. Zaghib. Recent development in carbon-LiFePO4 cathodes for lithium-ion batteries: A mini review. *Batteries*, **2022**, *8*(10), 133. https://doi.org/10.3390/batteries8100133
10. J. Tian, R. Xiong, W. Shen, and J. Lu. State-of-charge estimation of $LiFePO_4$ batteries in electric vehicles: A deep-learning enabled approach. *Appl. Energy*, **2021**, *291*, 116812. https://doi.org/10.1016/j.apenergy.2021.116812
11. J. Kumar, R. R. Neiber, J. Park, R. Ali Soomro, G. W. Greene, S. Ali Mazari, H. Young Seo, J. Hong Lee, M. Shon, D. Wook Chang, and K. Yong Cho. Recent progress in sustainable recycling of $LiFePO_4$-type lithium-ion batteries: Strategies for highly selective lithium recovery. *Chem. Eng. J.*, **2022**, *431*, 133993. https://doi.org/10.1016/j.cej.2021.133993
12. T. Shirane. Structure and physical properties of lithium iron oxide, $LiFeO_2$, synthesized by ionic exchange reaction. *Solid State Ionics*, **1995**, *79*, 227-233. https://doi.org/10.1016/0167-2738(95)00066-f
13. J. Zheng, J. A. Lochala, A. Kwok, Z. D. Deng, and J. Xiao. Research progress towards understanding the unique interfaces between concentrated electrolytes and electrodes for energy storage applications. *Adv. Sci.*, **2017**, *4*(8), 1700032. https://doi.org/10.1002/advs.201700032
14. Y. S. Lee, S. Sato, Y. K. Sun, K. Kobayakawa, and Y. Sato. A new type of orthorhombic $LiFeO_2$ with advanced battery performance and its structural change during cycling. *J. Power Sources*, **2003**, *119-121*, 285-289. https://doi.org/10.1016/s0378-7753(03)00152-6
15. Y. S. Lee, S. Sato, M. Tabuchi, C. S. Yoon, Y. K. Sun, K. Kobayakawa, and Y. Sato. Structural change and capacity loss mechanism in orthorhombic $Li/LiFeO_2$ system during cycling. *Electrochem. Commun.*, **2003**, *5*(7), 549-554. https://doi.org/10.1016/s1388-2481(03)00118-8
16. R. Kanno, T. Shirane, Y. Kawamoto, Y. Takeda, M. Takano, M. Ohashi, and Y. Yamaguchi. Synthesis, structure, and electrochemical properties of a new lithium iron oxide, $LiFeO_2$, with a corrugated layer structure. *J. Electrochem. Soc.*, **1996**, *143*(8), 2435-2442. https://doi.org/10.1149/1.1837027
17. R. Kanno, T. Shirane, Y. Inaba, and Y. Kawamoto. Synthesis and electrochemical properties of lithium iron oxides with layer-related structures. *J. Power Sources*, **1997**, *68*(1), 145-152. https://doi.org/10.1016/s0378-7753(96)02625-0
18. J. Li, J. Li, J. Luo, L. Wang, and X. He. Recent advances in the $LiFeO_2$-based materials for Li-ion batteries. *Int. J. Electrochem. Sci.*, **2011**, *6*(5), 1550-1561. https://doi.org/10.1016/s1452-3981(23)15092-9
19. H. J. Majeed, T. J. Idrees, M. A. Mahdi, M. J. Abed, M. Batool, S. R. Yousefi, A. Thumma, and L. S. Jasim. Synthesis and application of novel sodium carboxy methyl cellulose-g-poly acrylic acid carbon dots hydrogel nanocomposite (NaCMC-g-PAAc/ CDs) for adsorptive removal of malachite green dye. *Desalin. Water Treat.*, **2024**, *320*, 100822. https://doi.org/10.1016/j.dwt.2024.100822
20. M. Batool, M. N. Haider, and T. Javed. Applications of spectroscopic techniques for characterization of polymer nanocomposite: A review. *J. Inorg. Organomet. Polym. Mater.*, **2022**, *32*(12), 4478-4503. https://doi.org/10.1007/s10904-022-02461-3
21. M. Monajjemi and F. Mollaamin. Development of solid-state lithium-ion batteries (LIBs) to increase ionic conductivity through interactions between solid electrolytes and anode and cathode electrodes. *Energies*, **2024**, *17*(18), 4530. https://doi.org/10.3390/en17184530

22. F. Mollaamin, S. Shahriari, and M. Monajjemi. Influence of transition metals for emergence of energy storage in fuel cells through hydrogen adsorption on the MgAl surface. *Russ. J. Phys. Chem. B*, **2024**, *18*(2), 398-418. https://doi.org/10.1134/s199079312402026x
23. M. Monajjemi, F. Mollaamin, S. Shahriari, Z. Khalaj, H. Sakhaeinia, and A. Alihosseini. Interaction of nano-boron nitride sheets with electrodes in lithium ion battery for increasing voltage and amperage. *Russ. J. Phys. Chem. B*, **2024**, *18*(4), 1090-1112. https://doi.org/10.1134/s1990793124700465
24. F. Mollaamin. Competitive intracellular hydrogen-nanocarrier among aluminum, carbon, or silicon implantation: A novel technology of eco-friendly energy storage using research density functional theory. *Russ. J. Phys. Chem. B*, **2024**, *18*(3), 805-820. https://doi.org/10.1134/s1990793124700131
25. S. Shahriari, F. Mollaamin, and M. Monajjemi. Increasing the performance of {[(1–*x*–*y*)$LiCo_{0.3}Cu_{0.7}$](Al and Mg doped)]O_2}, *x*Li_2MnO_3, *y*$LiCoO_2$ composites as cathode material in lithium-ion battery: synthesis and characterization. *Micromachines*, **2023**, *14*(2), 241. https://doi.org/10.3390/mi14020241
26. F. Mollaamin and M. Monajjemi. Nanomaterials for sustainable energy in hydrogen-fuel cell: Functionalization and characterization of carbon nano-semiconductors with silicon, germanium, tin or lead through density functional theory Study. *Russ. J. Phys. Chem. B*, **2024**, *18*(2), 607-623. https://doi.org/10.1134/s1990793124020271
27. M. Monajjemi, F. Mollaamin, P. T. Thu, M. Otadi, A. Alihosseini, D. T. M. Dung, and D. M. Chien. Electrochemical investigation of lithium ion battery including $LiCo_{0.8}Ni_{0.2}O_2$, Li_2MnO_3, $LiNiO_2$ cathode materials. *Russ. J. Electrochem.*, **2020**, *56*(8), 669-679. https://doi.org/10.1134/s1023193520030076
28. F. Mollaamin and M. Monajjemi. Application of smart condensed H-adsorption nanocomposites in batteries: Energy storage systems and DFT computations. *Computation*, **2024**, *12*(12), 234. https://doi.org/10.3390/computation12120234
29. M. Monajjemi. Graphene/(h-BN) n/X-doped graphene as anode material in lithium ion batteries (X = Li, Be, B and N). *Maced. J. Chem. Chem. Eng.*, **2017**, *36*(1), 101. https://doi.org/10.20450/mjcce.2017.1134
30. F. Mollaamin. Designing novel nanomaterials for Li-ion batteries: A physico-chemical study through hydrogen-powered horizons. *New Mater. Compd. Appl.*, **2024**, *8*(3), 303-323. https://doi.org/10.62476/nmca83303
31. G. M. Ehrlich. Lithium-ion batteries. In: Handbook of Batteries / Eds. D. Linden, T.B. Reddy. New York, USA: McGraw-Hill, **2002**, Ch. 35.
32. Z. Yang, J. Zhang, M. C. W. Kintner-Meyer, X. Lu, D. Choi, J. P. Lemmon, and J. Liu. Electrochemical energy storage for green grid. *Chem. Rev.*, **2011**, *111*(5), 3577-3613. https://doi.org/10.1021/cr100290v